

## Structural arrest and dynamic localization in biocolloidal gels

N. Mahmoudi<sup>†‡\*</sup> and A. Stradner<sup>‡\*</sup>

Received 00th January 20xx,  
Accepted 00th January 20xx

DOI: 10.1039/x0xx00000x

[www.rsc.org/](http://www.rsc.org/)

### GFVT calculation

In the presence of non-adsorbing PEO, Casein micelles are driven towards each other by depletion attraction, and the strength of this attraction is given by the polymer concentration in the free volume  $c_{fv}$  and the overlap volume. By incorporating the correct dependence of the depletion thickness and osmotic pressure on polymer concentration, the generalized free volume theory (GFVT) allows for the determination of the effective colloid pair potential for any polymer concentration up to and including the semi-dilute regime. The GFVT then calculates the interaction potential  $U$  at contact using:<sup>1</sup>

$$-U/k_B T = \delta^2 \left( \delta + \frac{3}{2} \right) \delta_R^{-3} y (1 + 3.77y^{1.31}) \quad (S1)$$

where  $\delta_R = R_g/R$ ,  $y = c_{fv}/c^*$ , with  $c^*$  the overlap concentration of the polymer.  $\delta = \Delta/R$  is the relative width of the depletion layer ( $\Delta$ ) around a colloidal particle. The GFVT<sup>2</sup> describes the width of this layer as decreasing with increasing  $c$ , from  $R_g$  in the dilute regime to  $\xi$  in the semi-dilute regime where  $\xi \sim c_{fv}^{-\nu}$ <sup>3, 4</sup>. Fler and Tuinier<sup>1, 2</sup> captured the concentration-dependent decrease of the depletion layer width in this expression:

$$\delta = 0.865 \delta_R^{0.88} (1 + 3.95y^{2\nu})^{-0.44} \quad (S2)$$

Where  $\nu$  is the exponent for excluded-volume chains,  $\nu = 0.77$ .

We calculate  $c_{fv}$  from the total polymer concentration  $c$  in the mixture using  $c_{fv} = \alpha c$ , where  $\alpha$  is the fraction of free volume available to the polymer.  $\alpha$  is calculated using the standard scaled-particle result:<sup>5</sup>

$$\alpha = (1 - \phi) e^{(-A\gamma - B\gamma^2 - C\gamma^3)} \quad (S3)$$

where  $\gamma = \phi/(1 - \phi)$ ,  $A = 3\delta + 3\delta^2 + \delta^3$ ,  $B = 9\delta^2/2 + 3\delta^3$ ,  $C = 3\delta^3$ .

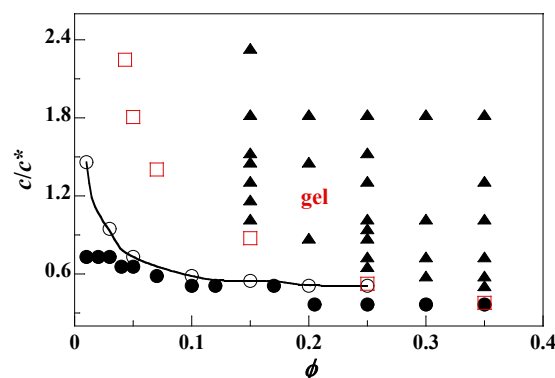


Fig. S1 Experimental state diagram for casein micelle-polyethylene oxide mixtures with polymer-to-colloid size ratio  $\delta \approx 0.31$ . Circles correspond to the fluid-fluid coexistence. Triangles correspond to gels studied in this work and determined by their rheology, dynamics and structural features as shown in Fig. 2 in the main manuscript. The solid line is a guide to the eye. Empty squares correspond to threshold  $\phi_g$ , and threshold  $c/c^*$ ,  $c_g/c^*$ , determined from scaling rheology data along  $U$ - and  $\phi$ -cuts. Filled black circles correspond to homogeneous fluid samples as investigated in <sup>6</sup>.

<sup>‡</sup> Adolphe Merkle Institute, University of Fribourg, Route de l'ancienne Papeterie 1, Marly, Switzerland.

<sup>‡</sup> Physical Chemistry, Lund University, Getingevägen 60, Lund, Sweden.

<sup>†</sup> Current address: ISIS Facility, STFC, Rutherford Appleton Lab., Harwell Science & Innovation Campus, Didcot, OX11 0QX, U.K.

\* Email: [naJET.mahmoudi@stfc.ac.uk](mailto:naJET.mahmoudi@stfc.ac.uk), [anna.stradner@fkem1.lu.se](mailto:anna.stradner@fkem1.lu.se)

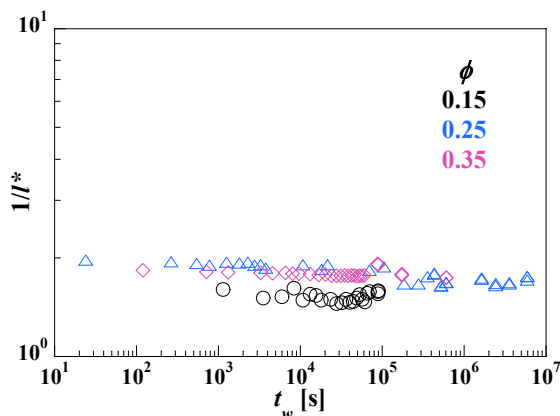


Fig. S2 Temporal evolution of the inverse of the photon transport mean free path,  $1/l^*$ , for casein-PEO mixtures at different  $\phi$  and  $U \sim -9 k_B T$ .

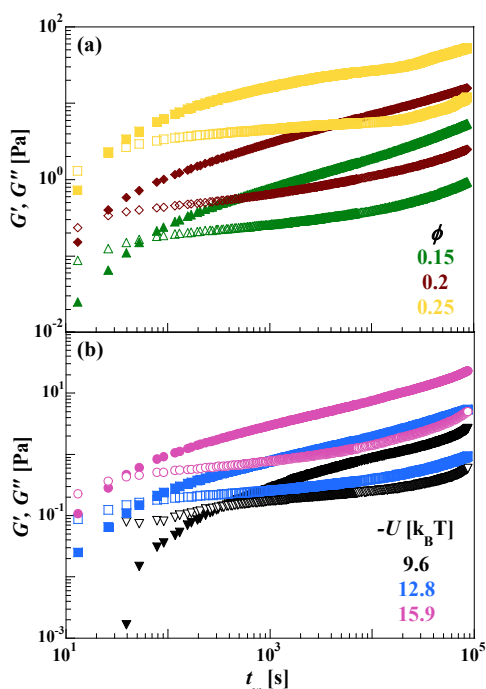


Fig. S3 Temporal evolution of storage (filled symbols) and loss (open symbols) moduli in the linear regime at  $\omega = 1$  rad/s and 1%-strain amplitude at (a) different  $\phi$  for  $U \approx -13 \pm 0.5 k_B T$ , and (b) at various  $U$  for  $\phi = 0.15$ . For clarity, only three  $\phi$  (a) (b) are shown.

### $\phi_g$ and $U_g$ determination

We find that the plateau elastic modulus grows in a critical fashion, with  $G_f \propto (\phi - \phi_g)^\nu$ , where for example for  $U \approx -13 \pm 0.5 k_B T$ , we obtain  $\phi_g = 0.043$  (Fig. S4a). Normalizing the reduced volume fraction by its critical value,  $\phi_g$ , collapses data at different  $U$ -values on a master curve as seen in Fig. 4a. This allows us to accurately determine the critical values of the volume fraction (in the low volume fraction branch of the phase diagram,  $\phi < 0.1$ ),  $\phi_g$ , for the fluid to solid transition. The dependence of the plateau modulus on  $U$  exhibits a similar critical behaviour (Fig. S4b), allowing us the same accurate determination of the critical values of the interaction potential

(high volume fraction part of the phase diagram,  $\phi \geq 0.15$ ),  $U_g$ , where the fluid to solid transition occurs.

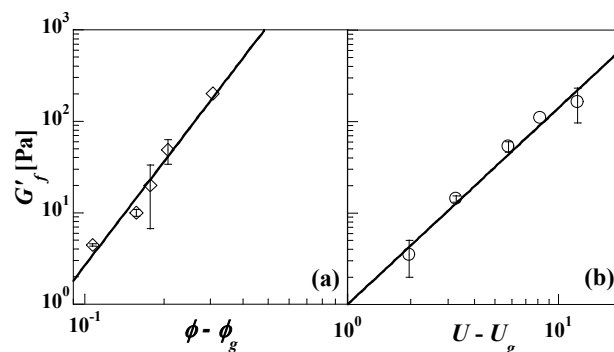


Fig. S4 Dependence of the elastic plateau modulus on the reduced volume fraction for an interaction potential  $U \approx -13 \pm 0.5 k_B T$  (a), and on the reduced interaction potential for a volume fraction  $\phi \approx 0.35$  (b). The solid lines are fits of the experimental data to  $G_f \propto (\phi - \phi_g)^\nu$ .

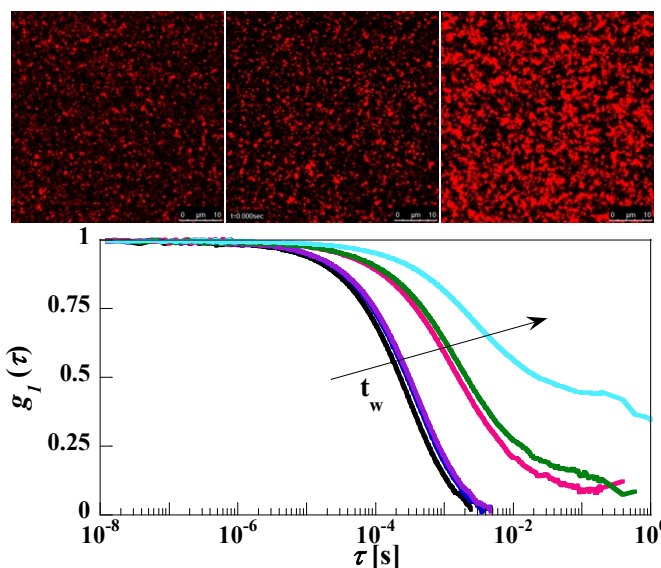


Fig. S5 Coarsening of casein-PEO structure with time for a shallow quench,  $\phi = 0.3$  for  $U \approx -6 k_B T$ , from clusters of a few particle diameters at  $t_w = 5$  min (left image) and  $t_w = 14$  min (middle image) to a bicontinuous spinodal structure at  $t_w = 27$  h (right image), and the corresponding transition from ergodic-to-non-ergodic dynamics.

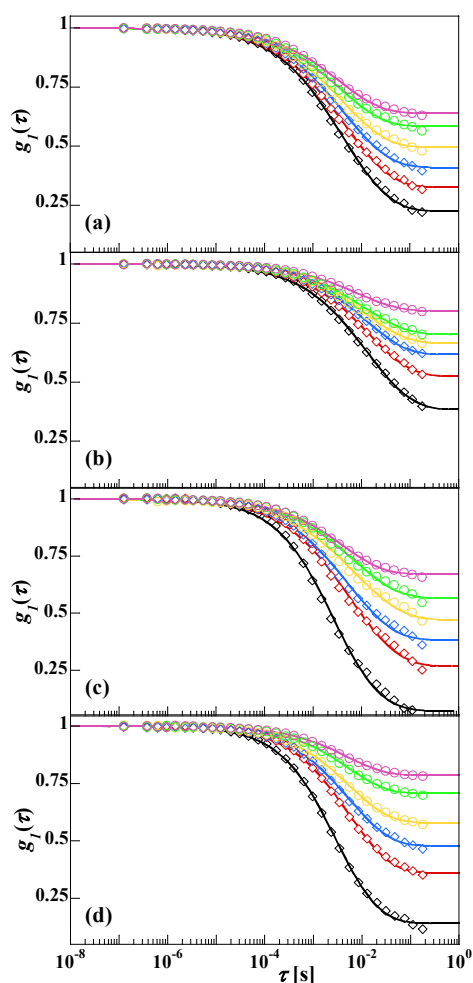


Fig. S6 DWS intermediate scattering functions,  $g_1(\tau)$ , as a function of  $t_w$ , increasing from bottom to top, and the corresponding stretched-exponential decay fits (solid lines) using Eq. 7, for casein-PEO at: (a)  $\phi = 0.2$  and  $U \approx -13 k_B T$ , (b)  $\phi = 0.15$  and  $U \approx -9 k_B T$ , (c)  $\phi = 0.25$  and  $U \approx -9 k_B T$ , and (d)  $\phi = 0.35$  and  $U \approx -9 k_B T$ .

### Fractal gel model inapplicability

Following the approach of Romer et al.<sup>6</sup> and Krall and Weitz<sup>7</sup>, and using the dynamical data at low volume fractions ( $0.15 \leq \phi \leq 0.22$ ), we determine the fractal dimension  $d_f$  and  $\beta = 2\varepsilon + d_B \leq 11/3$ , a parameter that depends on the characteristics of the stress-bearing strands, where  $1 \leq d_B \leq 5/3$  is the backbone bond dimension and  $0 \leq \varepsilon \leq 1$  describes the dimension of the chain projected on a plane perpendicular to the line connecting the ends of the chain.<sup>8</sup> In Fig. S6, we show the  $\phi$  dependence of the squared localization length  $\Delta^2$  (black circles) and the normalized fast relaxation time  $D_0 \tau_f$  (blue circles) at  $U \approx -13 \pm 0.5 k_B T$ , where we multiply  $\tau_f$  by the free diffusion coefficient of casein micelles,  $D_0 = k_B T / 6\pi\eta R$ , to account for differences in the background viscosity. A power law is observed for both  $\Delta^2$  (black solid line) and  $D_0 \tau_f$  (blue dashed line). Krall and Weitz's model predicts that:<sup>7</sup>

$$\Delta^2 \propto \phi^{-\beta/(3-d_f)} \quad (S4)$$

$$\tau_f \propto \phi^{-(\beta+1)/(3-d_f)}$$

(S5)

Combining Eq. (S4) and (S5), we determine  $d_f$  by fitting  $\tau_f D_0 / \Delta^2 \propto \phi^{-1/(3-d_f)}$ .

As expected from the fitted exponents (equations on the Fig. S6), the value extracted is negative (-4.3) compared to the experimental values coarsely determined from CLSM ranging from 1.8 to 2.6. The fitted values of  $d_f$  and  $\beta$  are not physically meaningful confirming the breakdown of the fractal gel model at  $\phi > 0.1$ .

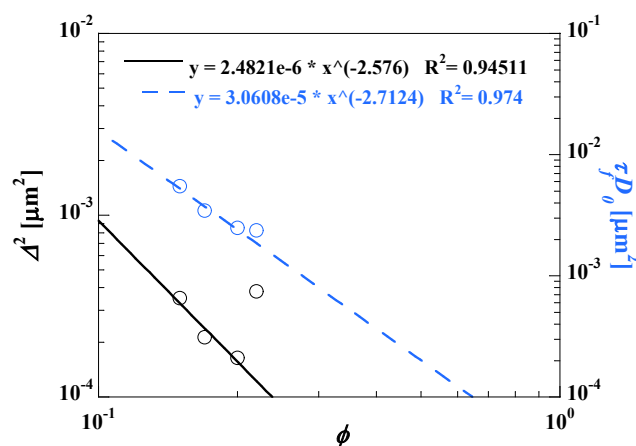


Fig. S7 the squared localization length  $\Delta^2$  (black circles) and normalized fast relaxation time  $D_0 \tau_f$  (blue circles) of casein-PEO gels as a function of the volume fraction  $\phi$ , for an interaction potential  $U \approx -13 \pm 0.5 k_B T$ . The black solid line and blue dashed line are fits to Eq. (S4) and (S5), respectively.

### References

1. G. J. Fleer and R. Tuinier, *Adv. Colloid Interface Sci.*, **2008**, *143*, 1-47.
2. G. J. Fleer and R. Tuinier, *Phys. Rev. E: Stat., Nonlinear, Soft Matter Phys.*, **2007**, *76*, 041802.
3. G. J. Fleer, A. M. Skvortsov and R. Tuinier, *Macromol. Theory Simul.*, **2007**, *16*, 531-540.
4. P.-G De Gennes, *Scaling concepts in polymer physics*. Cornell University Press: Ithaca, 1979.
5. H. N. W. Lekkerkerker, W. C. K. Poon, P. N. Pusey, A. Stroobants and P. B. Warren, *Europhys. Lett.*, **1992**, *20*, 559-564.
6. N. Mahmoudi and A. Stradner, *J. Phys. Chem. B*, 2015, **119**, 15522-15529.
7. S. Romer, H. Bissig, P. Schurtenberger and F. Scheffold, *Europhys. Lett.*, 2014, **108**, 48006.
8. A. H. Krall and D. A. Weitz, *Phys. Rev. Lett.*, 1998, **80**, 778.
9. R. de Rooij, D. van den Ende, M. H. G. Duits and J. Mellema, *Phys. Rev. E: Stat., Nonlinear, Soft Matter Phys.*, 1994, **49**, 3038-3049.

